

ENHANCED PHOTOCATALYTIC DEGRADATION OF TETRACYCLINE BY TiO_2 NANOTUBES COATED WITH TiO_2 NANOFIBERS

Roberta IRODIA¹

The focus of this work is on the electrochemical synthesis of photocatalytic electrodes based on TiO_2 nanostructures on Ti thin film and their efficiency in the degradation of tetracycline aqueous solution. In this study it was demonstrated that the surface characteristics of the developed photocatalyst have a very important influence on its optical and photocatalytic properties. This behavior was supported by correlation between the results from scanning electron microscopy and UV-Vis light technologies. Good performance was seen for the photocatalytic degradation of tetracycline in water using the manufactured TiO_2 nanotubes coated with TiO_2 nanofibers from suspension. This method may be applicable to the decomposition of other organic pollutants with the same chemical structures.

Keywords: Antibiotics, Nanostructures, TiO_2 nanotubes, TiO_2 nanofibers

1. Introduction

Numerous studies are based on environmental protection and the main focus is on finding many ecological methods to treat and protect the environment. One of the biggest world concerns are based on the water pollution which is largely caused by global industrialization. This is why experts are searching for numerous methods to conserve natural waters by re-treating wastewater [1].

Advanced oxidation processes involves wastewater pollutants removal and among them photocatalysis it is known to be promising in pollutants degradation by using metal semiconductors [1, 2]. As a photocatalyst, TiO_2 stands out for its increased efficiency of organic pollutants degradation and has also economical advantages, is stable and nontoxic [3]. Titanium dioxide is employed in a variety of processes, such as dye-sensitized solar cells, photocatalysis, gas sensing, self-cleaning, and antimicrobial applications [4,5]. Due to this, there has been made many studies on creating TiO_2 nanostructures with carefully regulated morphologies [4]. TiO_2 catalyst is capable of inactivating, attacking microorganism with reactive oxygen species and in the presence of UV light irradiation pairs electrons are produced.

¹ Dept. of General Chemistry, University POLITEHNICA of Bucharest, Romania, e-mail: roberta.irodia@upb.ro

There is also a weak point in using TiO_2 due to the fact that the length of the band gap is about 3.2 eV so this means that the pure TiO_2 can be activated only by irradiation under the UV light so it can absorb only 7% of visible light found in spectrum making TiO_2 less efficient [5].

However, there are studies that demonstrate several strategies to extend the spectral band of TiO_2 into the visible range by employing dopants such as metals, oxides, or nanostructures, hence increasing the photocatalytic efficacy of this semiconductor.

Numerous types of nanostructured TiO_2 have been created, including nanocrystallite, nanoparticles, elongated nanotubes, nanosheets, nanorods, nanocolumn arrays, and nanofibers. These nanostructures were successfully created using a number of different techniques, including the template method, sol-gel methods, hydrothermal processes, and the anodic oxidation method [6]. TiO_2 nanoparticles are widely used in photocatalysis process, although the nanoparticles recovery involves expansive separation processes [2]. Nanofibers (NFs) have the advantages of absorbing a large amount of UV light and this is the reason why NFs are most used in wastewater treatments [7] while nanotubes have a larger surface area and presents biological performances such as antibacterial activity, organic compounds photocatalytic degradation so this will be helpful in obtaining clean water [8].

In recent decades, antibiotics have been utilized intensively in medicinal therapy and agricultural activities, gaining interest. Antibiotics are vital to human health, but their widespread usage has an unintended side effect: their accumulation in ecosystems [9].

One of the most commonly used antibiotics in medicine are Tetracyclines (TCs) and most of them are eliminated through feces and urine as unmetabolized compounds as a result of their poor absorption. TCs, are the second most extensively used class of antibiotics, and are used in a variety of applications such as veterinary medicine, aquaculture[10]. The development of antibiotic-resistant bacterial strains that are invulnerable to the currently available medications is the most hazardous effect of antibiotics on the environment [11]. The development of antimicrobial resistance in microorganisms observed against TC is caused by the slow rate of degradation and high persistence of antibiotics in the environment. This could result in the extinction of some species, disrupting the ecological equilibrium [12, 13]. The photocatalytic degradation of TC in aqueous solution was examined in this study involving TiO_2 nanotubes and coated with TiO_2 nanofibers as the photocatalyst under UV irradiation.

In this work it has been demonstrated that the deposition method of TiO_2 nanofibers synthesized by electrospinning method on anodized TiO_2 nanotubes has a great influence on the surface properties influencing the optical and photocatalytic character.

2. Experimental part

a. Materials and methods

Initial pretreatment

Titanium (Ti) plates are first mechanically polished using Buehler papergrit of different sizes, 320, 800, 1200 and after polishing, Ti plates are cleaned by ultrasounds as follows: 15 minutes in deionized water, 15 minutes ethanol and 15 minutes acetone [14].

Electrochemical anodization

TiO_2 nanotubes (TiO_2 -NTs) were prepared as found in literature [15] by anodization using the pretreated Ti plate as working electrode with the size of 2,5 cm^2 and a graphite as a counter electrod, keeping the working distance between those 2 electrod for 2 cm. The electrolyte solution contains a mixture of 0,4 wt. % NH_4F (Sigma Aldrich), 2wt. % ultrapure H_2O and ethylenglycol (EG) (Sigma Aldrich) .

The anodization was made using a laboratory DC power suply (Matrix) at 30 V during 3 h and after this process took place, annealing is performed at 450 °C for 2 h in order to obtain a better cristalinity phase of TiO_2 .

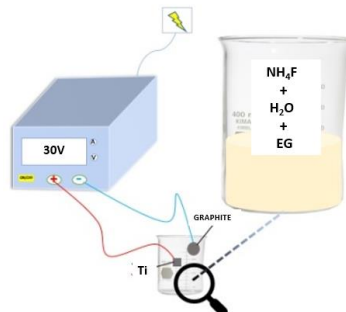


Fig. 1. Laboratory anodization equipment

Electrospinning process

In order to obtain TiO_2 nanofibers (TiO_2 -NFs), it is necessary to prepare a precursor consisting of a polyvinylpyrrolidone PVP (Alfa Aesar) carrier polymer, an alkoxide precursor such as Titanium Butoxide (IV) (Sigma Aldrich) and a mixture in a molar ratio 1:1 N,N dimethylformamide DMF (Alfa Aesar) and isopropanol (Alfa Aesar), following to add a known amount of glacial acetic acid (Alfa Aesar). The sample was magnetically stirred for about 4-5 h and the solution is used therefor as a precursor for electrospinning.

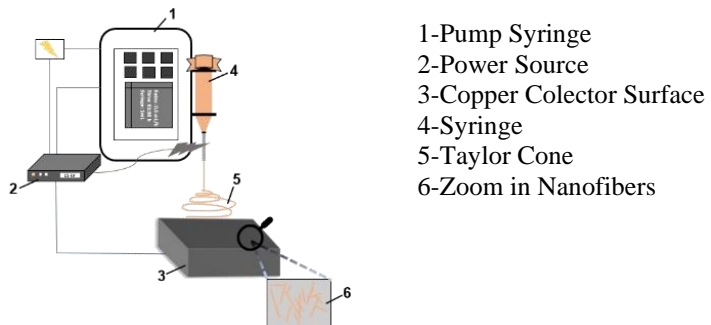


Fig. 2. Laboratory electrospinning equipment

There are four important parameters which we must take care of, such as the distance from the tip of the syringe needle to the collector plate, the setting of a deposition time from the syringe on the collector plate, the applied voltage and the flow rate. Therefore, the syringe which contains the precursor solution is positioned in the injection pump and is connected straight to the high voltage DC power supply. The collector is positioned taking into account the distance from the tip of the needle. Operating parameters are setted at 20 V, distance from the tip of the needle to collector of 20 cm, flow rate of 0,5 mL/h and the required time of 1,5 h. After fixing the nanofibers on the surface, the nanofibers are calcined at a temperature of 500 °C for 4 hours. At a temperature of 300-400 °C, water and -OH groups from the solution are eliminated. In the TiO₂ system, the anatase phase will pass around the temperature of 350-400 °C, and the rutile phase starts at 500-600 °C, depending on the shape of the materials [16].

b. Photocatalytic test

In order to perform photocatalytic testing, sample is placed into 10 mL of Tetracycline hydrochloride aqueous solution (TC), which has a initial concentration of 5 mg/L. The solution was then vigorously stirred for 30 minutes in dark conditions to bring it to adsorption-desorption equilibrium. A mercury vapor lamp is used as visible light source, and was used to perform the photocatalytic test. Between the optical source and the entire experimental setup, there were no filters. In order to eliminate the effects of lamplight from the outside world, the entire system was constructed as an enclosed box. Photocatalytic test was performed during 240 minutes under stirring and visible light irradiation. Samples were taken every 10 minutes and analyzed using UV-Vis Spectrophotometer JENWAY 6715 to measure the concentration of TC degradation in time.

3. Results and discussion

3.1. Deposition process

A. In order to obtain TiO_2 nanotubes coated with TiO_2 nanofibers, a previously anodized titanium plate is taken and supposed to electrospinning. By fixing the plate on the collector plate, nanofibers are electrostatically attracted to the surface, thus creating adhesion between the active surface of TiO_2 Nanotubes and the obtained TiO_2 nanofibers. The samples are subjected to calcination at 450 °C for 4 hours in order to remove the carrier polymer. A new photocatalyst TiO_2 -NT/NF ES (TiO_2 -Nanotubes/Nanofibers coated by electrospinning) was obtained.

B. TiO_2 -NFs were detached from the surface by ultrasonication in distilled water making a nanofibers suspension which is introduced in a spray in order to attach NFs layer on the TiO_2 -NTs created before by anodization method. After spraying took place, the samples were introduced into the oven at 100 °C for half an hour, and so on this nanostructures TiO_2 -NT/NF S (TiO_2 -Nanotubes/Nanofibers coated by suspension) will improve the photocatalytic degradation efficiency.

3.2. Surface and optical measurements

SEM Characterization

Morphological evolution and the phase transformations of coated TiO_2 nanotubes can be seen by using SEM - scanning electron microscopy (SEM, FEI Quanta 650 FEG – Thermo Fisher Scientific, Waltham, MA, USA) at different magnifications.

TiO_2 -NT/NF ES

Surface morphologies of TiO_2 -NT/NF ES prepared by anodization followed by electrospinning and calcination at 450 °C have been studied by SEM. In the following SEM images (Fig.3) can be clearly observed TiO_2 NTs and TiO_2 NFs presence on Ti plate. This images shows ordered nanostructures that presents many active sites on the surface. The distribution of TiO_2 NTs and TiO_2 NFs on the surface is uniform and the nanofibers appear to be like a cap for the nanotubes, slightly covering the nanotubes.

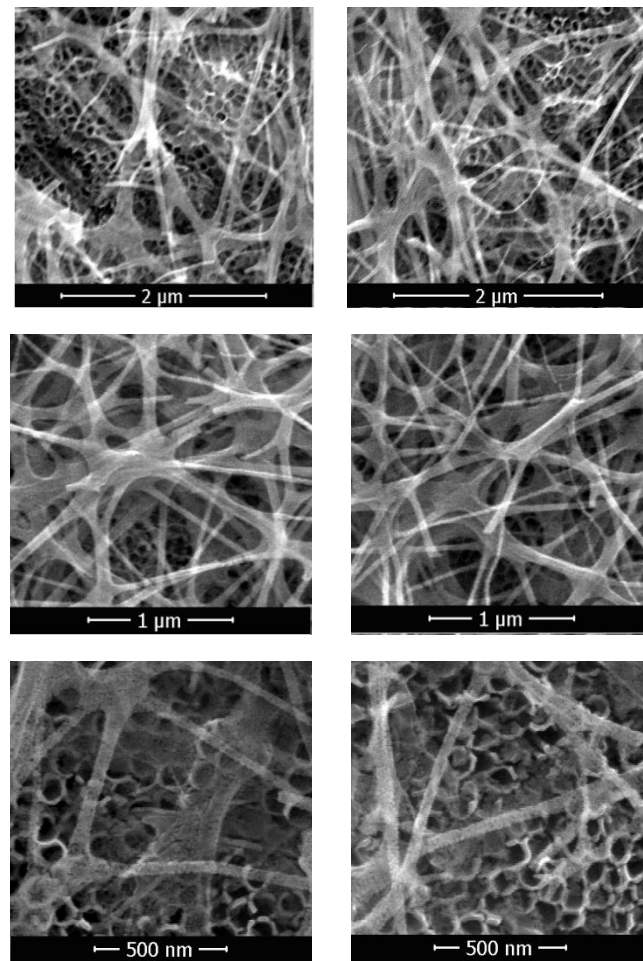


Fig.3. SEM images at different magnifications of TiO_2 -NT/NF ES

TiO_2 -NT/NF S

As can be seen from this SEM figure below TiO_2 -NTs were uniformly distributed on the entire sample surface of a Ti plate over which TiO_2 -NFs have been sprayed. The surface consist of a well-organized and homogeneous arrangement of TiO_2 -NTs with an average diameter of 80 nm.

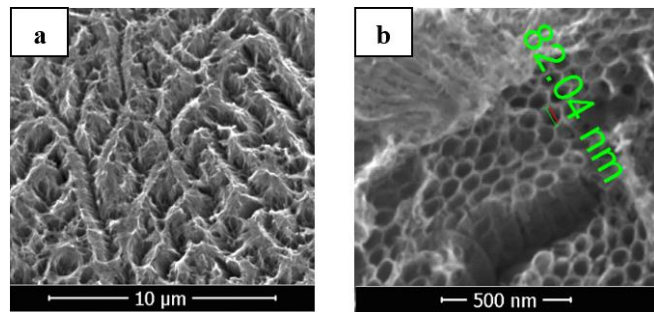


Fig. 4. Top view of SEM images of a) TiO_2 -NTs coated with TiO_2 -NFs seen at $10 \mu\text{m}$ b) TiO_2 -NTs coated TiO_2 -NFs seen at 500 nm

Following the dehydration process of the samples, TiO_2 -NFs were attached to the surface forming some agglomerates on certain parts, these things being well observed through SEM images. It is observed that above these nanotubes there is still a fatty film that needs to be removed to create a better adhesion.

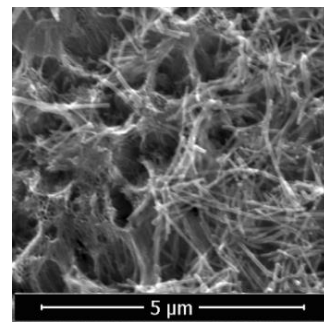
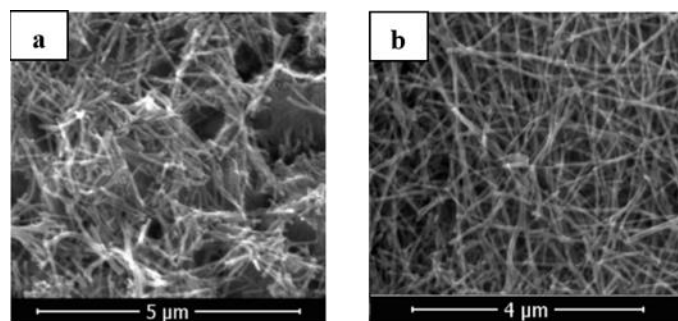


Fig. 5. Top view of SEM image of TiO_2 -NTs/NFs seen at $5 \mu\text{m}$

Despite the deposition of the TiO_2 -NFs on the nanotubes, there are observed areas of the surface on which there are no TiO_2 -NFs, which indicates that the fatty film from the surface of the TiO_2 -NTs influences their ability to create adhesion.



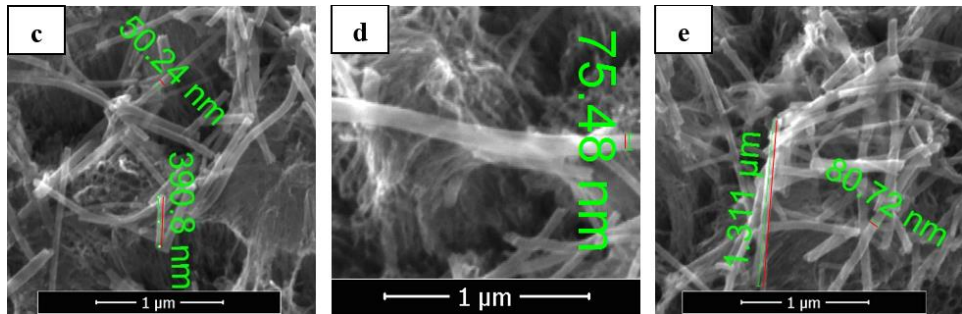


Fig. 6. Distribution of TiO_2 -NTs/NFs observed in SEM images a) 5 μm b) 4 μm c,d,e) 1 μm

The NFs length varies from 390 nm to 1,314 micrometers and the outer diameter varies from 50-75 nanometers. It can be observed that the NFs have different length due to the ultrasound process by which the nanofibers were broken and detached from the Ti plate.

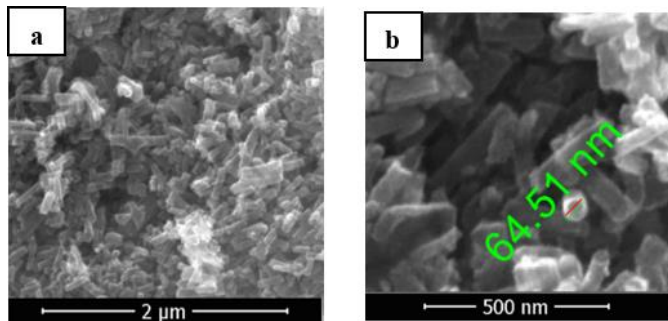


Fig. 7. SEM images - distribution of broken a) TiO_2 -NFs seen at 2 μm b) TiO_2 -NFs having different lengths between 64 seen at 500 nm

Large surfaces were covered with broken NFs structures. In the above SEM images can be seen the back and the remains of the nanofibers detached by ultrasound. Those areas do not have nanotubes because the anodization occurred only on a half of side of the Ti plate. So an interesting thing it's that when broken TiO_2 -NFs are sprayed on the surface, long TiO_2 -NFs make adhesion with nanotubes and the back-remains are headed to that plain area forming agglomerates.

Optical measurements. Band-gap energy

The reflectance spectra captured by the Perkin Elmer Lambda 950 UV-Vis spectrophotometer were recorded in order to determine the band gap energy of the samples. As reported in the literature and previous studies, TiO_2 nanotubes have a band gap energy of 3.4 eV which is a little higher than the anatase phase of TiO_2 which is about 3.2 eV. The size effect and the cristalinity phase of the TiO_2 semiconductor in the nanostructure is most likely a reason to visible reduce band gap energy [17].

In the study of energy and the environment, TiO_2 anatase is crucial. TiO_2 's high bandgap of 3.2 eV is a significant obstacle to the development of artificial photosynthesis since it limits the light it can absorb to the UV range. TiO_2 -based photocatalysis could develop into a competitive renewable energy source if the bandgap of anatase could be lowered to the visible spectrum. Here, we report the identification of TiO_2 anatase nanosurface with a decreased bandgap that improve activation of the solar spectrum region [18].

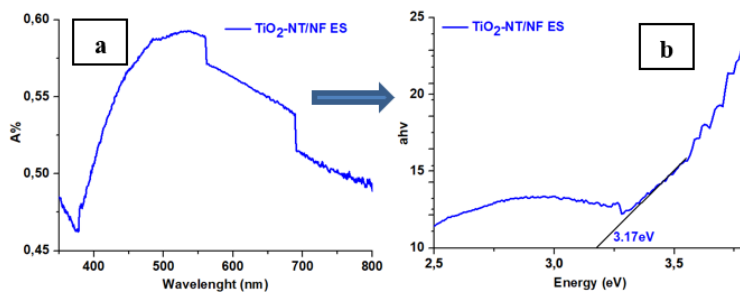


Fig. 8. a) UV-Vis spectrum of TiO_2 -NT/NF ES b) Tauc plot diagram and band gap energy of TiO_2 -NT/NF ES

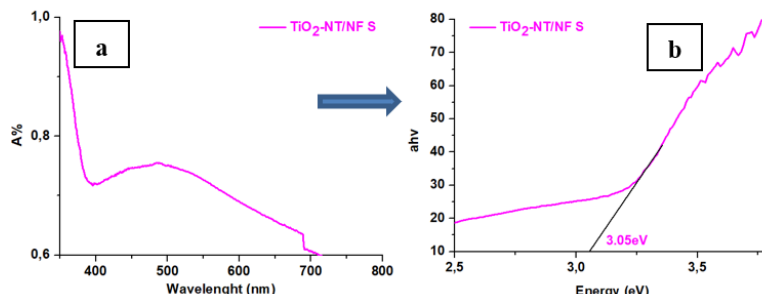


Fig. 9 a) Recorded UV-Vis spectrum of TiO_2 -NT/NF S b) Tauc plot and band gap energy of TiO_2 -NT/NF S

From Fig. 8. and Fig. 9. comparing the two samples, a decreased band gap energy is well observed this is clearly due to methods of depositing TiO_2 nanofibers on the previously anodized sub-shelf. Correlating the band gap energy values (see Table 1):

Table 1

Band gap energy values found from Tauc's Plot

Catalysts	Band gap Energy, eV
TiO_2 -NT/NF ES	3.17
TiO_2 -NT/NF S	3.05

and the SEM images, we can conclude that the electrode showing broken (TiO₂-NT/NF S) has a larger contact surface and also helps in photocatalysis processes by reducing the band gap energy.

3.3.Evolution of photocatalytic degradation

An UV-Vis equipment operating at different wavelenghts was used to determine the concentration of TC at 360 nm. For the measurement of the concentration and amount of TC in the solution supposed to photocatalytic degradation, a standard calibration curve is needed and was performed using TC hydrochloride solution at several dilutions.

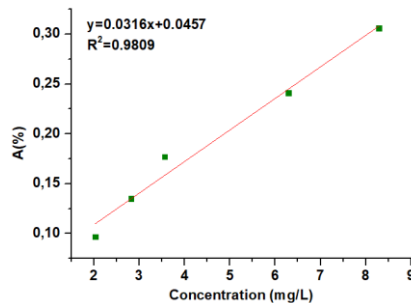


Fig. 10. Standard calibration curve at 5 TC concentrations

The coefficient of correlation, or R, or the coefficient of determination, or R^2 , are typically used to represent the calibration curve's linearity. A correlation coefficient close to one ($R = 1$) is adequate proof that the calibration curve is linear [19]. Further, the photodegradation of TC over TiO₂-NT/NF ES and TiO₂-NT/NF S was assessed under UV-Vis light irradiation. These studies were carried out three times each. According to Fig. 11, the amount of TC in solution is more decreasing with increasing light exposure time in the presence of TiO₂-NT/NF S (Fig. 11 b) catalytic surface, showing that photodegradation of TC reached 80% efficiency.

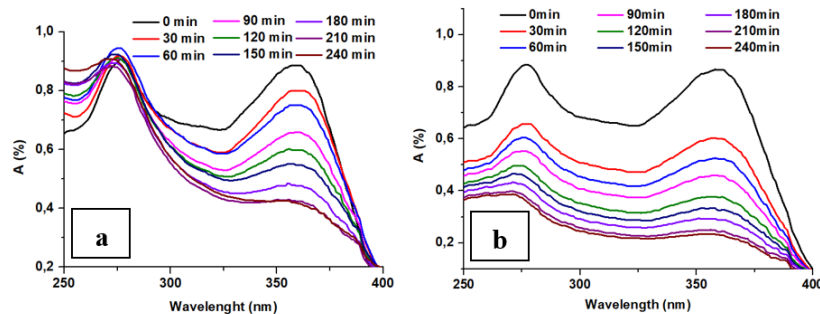


Fig. 11. UV-Vis spectrum showing photocatalytic degradation of TC during 240 minute a) photocatalytic degradation over TiO₂-NT/NF ES b) photocatalytic degradation over TiO₂-NT/NF S

These results show that the catalytic surface TiO_2 -NT/NF S is more efficient for the proposed application. Each experiment were carried out three times, and from Table 2 the absorbance values of TC degradation can be seen at the beginning of irradiation and after 240 minutes of irradiation. Standard deviation was calculated using absorbance values for each sample at different times. Moreover, the concentration of TC degradation in time was calculated relating to regression line obtained from calibration curve (see Fig. 10.)

Table 2

Absorbance values of TC degradation recorded at 360nm after 240 min of light exposure

Samples	Photocatalytic time, min	A%, $\lambda_{360\text{nm}}$	Standard Deviation
TiO_2 -NT/NF ES	0	0.886	± 0.004
	240	0.416	± 0.072
TiO_2 -NT/NF S	0	0.869	± 0.010
	240	0.233	± 0.086

With the estimation of the final concentration after time t , the kinetics of the photodegradation of TC by TiO_2 -NT/NF S photocatalyst under various conditions were studied. A graph based on first-order kinetics was utilized and constructed to adapt the reaction to the appropriate kinetics. Fig. 12 b) shows a graph of the first-order kinetics of the reaction between TC solution and TiO_2 -NT/NF S photocatalyst.

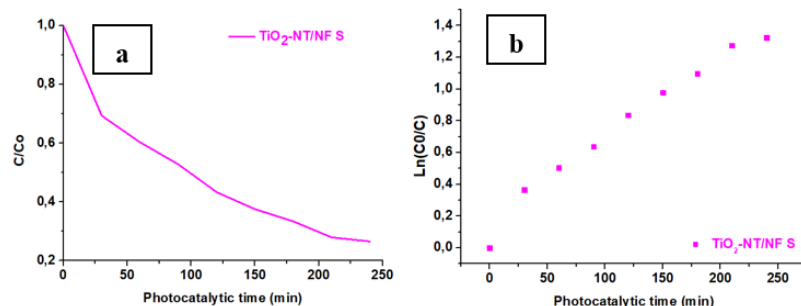


Fig. 12. a) TC photodegradation efficiency over TiO_2 -NT/NF b) First-order kinetics graph of photodegradation of TC with TiO_2 -NT/NF S photocatalyst.

Using a pseudo first order kinetic equation, it have been shown the behavior of catalyst when exposed to light, so according to Langmuir-Hinshelwood equation:

$$\ln\left(\frac{C_0}{C}\right) = k \times t \quad (1)$$

where C is the TC concentration at the time t and C_0 is the initial TC concentration, the apparent first-order rate constant, k , was calculated [20]. Fig. 12 also provides

the appropriate kinetic constants and regression coefficients for the photocatalysis of TC by TiO_2 . The rate constants of photodegradation of TC with TiO_2 -NT/NF S is $5.3 \cdot 10^{-3} \text{ min}^{-1}$, having a correlation coefficient of $R^2 = 0.9870$ (Table 3).

Table 3

Pseudo-first order model parameter for TC degradation		
Catalyst	Kinetic rate constants (k, min^{-1})	Correlation coefficient (R^2)
TiO_2 -NT/NF S	$5.3 \cdot 10^{-3}$	0.9870

4. Conclusions

The surface characteristics and optical properties are influenced by the method used for the deposition of TiO_2 -NF on TiO_2 -NT previously anodized on Ti foil. Two categories of photocatalysts based on TiO_2 -NT/NF were obtained, thus TiO_2 -NF were synthesized by electrospinning method and then deposited either directly on the TiO_2 -NT anodized substrate (TiO_2 -NT/NF ES) or by sputtering the TiO_2 -NF suspension obtained by ultrasonication (TiO_2 -NT/NF S). Both catalysts obtained showed ordered nanostructures with many surface active sites. The nanofibers are uniformly distributed on the anodized nanotubes, and the adhesion behavior depends on the presence of fatty films on the nanotube surface.

SEM images showed that the obtained photocatalysts have different structure and properties. Thus, TiO_2 -NT/NF S exhibited a larger contact area than TiO_2 -NT/NF ES, due to a better distribution of the broken TiO_2 -NFs obtained by the sonication process. This broken structure of the nanofibers led to a lower band gap value of about 3.05 eV.

The applicability in the photocatalytic degradation of TiO_2 -NT/NF S catalyst was demonstrated in the degradation of TC hydrochloride solution during 240 minutes of light irradiation. Note that the degradation took place almost completely, the absorbance peak of TC decreased from the initial absorbance of 0.869 and after 240 minutes of irradiation the final absorbance achieved the value of 0.233. So the degradation was effective and successfully. This catalytic surface is claimed to be a good photocatalytic surface in the degradation of drugs and organic compounds regarding the environmental protection.

Acknowledgement

- ✓ The SEM analyses was funded by European Regional Development Fund through Competitiveness Operational Program 2014–2020, Priority axis 1, Project No. P_36_611, MySMIS code 107066.
- ✓ This work has been funded by the European Social Fund from the Sectoral Operational Programme Human Capital 2014-2020, through the Financial Agreement with the title "Training of PhD students and postdoctoral

researchers in order to acquire applied research skills - SMART", Contract no. 13530/16.06.2022 - SMIS code: 153734.

R E F E R E N C E S

- [1]. X. Li, H. Lin, X. Chen, H. Niu, J. Liu, T. Zhang, and F. Qu, Dendritic alpha-Fe₂O₃/TiO₂ nanocomposites with improved visible light photocatalytic activity. *Phys Chem Chem Phys*. **18**(13): p. 9176-85. 2016
- [2]. C.B.D. Marien, T. Cottineau, D. Robert, and P. Drogui, TiO₂ Nanotube arrays: Influence of tube length on the photocatalytic degradation of Paraquat. *Applied Catalysis B: Environmental*. **194**: p. 1-6. 2016
- [3]. J. Qiu, F. Liu, C. Yue, C. Ling, and A. Li, A recyclable nanosheet of Mo/N-doped TiO₂ nanorods decorated on carbon nanofibers for organic pollutants degradation under simulated sunlight irradiation. *Chemosphere*. **215**: p. 280-293. 2019
- [4]. O.V. Otieno, E. Csáki, O. Kéri, L. Simon, I.E. Lukács, K.M. Szécsényi, and I.M. Szilágyi, Synthesis of TiO₂ nanofibers by electrospinning using water-soluble Ti-precursor. *Journal of Thermal Analysis and Calorimetry*. **139**(1): p. 57-66. 2020
- [5]. V. Etacheri, C. Di Valentin, J. Schneider, D. Bahnemann, and S.C. Pillai, Visible-light activation of TiO₂ photocatalysts: Advances in theory and experiments. *Journal of Photochemistry and Photobiology C: Photochemistry Reviews*. **25**: p. 1-29. 2015
- [6]. H.A.R.A. Hussain, M.A.M. Hassan, and I.R. Agool, Synthesis of titanium dioxide (TiO₂) nanofiber and nanotube using different chemical method. *Optik*. **127**(5): p. 2996-2999. 2016
- [7]. N. Singh, M.S. Rana, and R.K. Gupta, Modelling studies for photocatalytic degradation of organic dyes using TiO₂ nanofibers. *Environ Sci Pollut Res Int*. **25**(21): p. 20466-20472. 2018
- [8]. M. Bencina, I. Junkar, R. Zaplotnik, M. Valant, A. Iglic, and M. Mozetic, Plasma-Induced Crystallization of TiO(2) Nanotubes. *Materials (Basel)*. **12**(4). 2019
- [9]. X. Zhu, Y. Wang, and D. Zhou, TiO₂ photocatalytic degradation of tetracycline as affected by a series of environmental factors. *Journal of soils and sediments*. **14**(8): p. 1350-1358. 2014
- [10]. M. Cao, P. Wang, Y. Ao, C. Wang, J. Hou, and J. Qian, Visible light activated photocatalytic degradation of tetracycline by a magnetically separable composite photocatalyst: Graphene oxide/magnetite/cerium-doped titania. *Journal of Colloid and Interface Science*. **467**: p. 129-139. 2016
- [11]. X.-D. Zhu, Y.-J. Wang, R.-J. Sun, and D.-M. Zhou, Photocatalytic degradation of tetracycline in aqueous solution by nanosized TiO₂. *Chemosphere*. **92**(8): p. 925-932. 2013
- [12]. M. Sharma, M.K. Mandal, S. Pandey, R. Kumar, and K.K. Dubey, Visible-Light-Driven Photocatalytic Degradation of Tetracycline Using Heterostructured Cu₂O-TiO₂ Nanotubes, Kinetics, and Toxicity Evaluation of Degraded Products on Cell Lines. *ACS Omega*. **7**(37): p. 33572-33586. 2022
- [13]. Y. Ben, C. Fu, M. Hu, L. Liu, M.H. Wong, and C. Zheng, Human health risk assessment of antibiotic resistance associated with antibiotic residues in the environment: A review. *Environmental Research*. **169**: p. 483-493. 2019
- [14]. C. Dumitriu and C. Pirvu, Electrochemical studies on TiO₂ nanotubes modified Ti electrodes. *UNIVERSITY POLITEHNICA OF BUCHAREST SCIENTIFIC BULLETIN SERIES B-CHEMISTRY AND MATERIALS SCIENCE*. **74**(3): p. 93-106. 2012
- [15]. C. Dumitriu, M. Popescu, C. Ungureanu, and C. Pirvu, Antibacterial efficiencies of TiO₂ nanostructured layers prepared in organic viscous electrolytes. *Applied Surface Science*. **341**: p. 157-165. 2015

- [16]. C. Dumitriu, A.B. Stoian, I. Titorencu, V. Pruna, V.V. Jinga, R.-M. Latonen, J. Bobacka, and I. Demetrescu, Electrospun TiO₂ nanofibers decorated Ti substrate for biomedical application. *Materials Science and Engineering: C*. **45**: p. 56-63. 2014
- [17]. M. Razali, N.A. Ismail, and M. Yusoff, Study on Band Gap Energy of F Doped TiO₂ Nanotubes. *Materials Science Forum*. **889**: p. 234-238. 2017
- [18]. C. Dette, M.A. Pérez-Osorio, C.S. Kley, P. Punke, C.E. Patrick, P. Jacobson, F. Giustino, S.J. Jung, and K. Kern, TiO₂ anatase with a bandgap in the visible region. *Nano Lett.* **14**(11): p. 6533-8. 2014
- [19]. S.M. Moosavi and S. Ghassabian, Linearity of calibration curves for analytical methods: A review of criteria for assessment of method reliability. Vol. 109. 2018: IntechOpen Limited London, UK.
- [20]. S. Natarajan, H.C. Bajaj, and R.J. Tayade, Recent advances based on the synergetic effect of adsorption for removal of dyes from waste water using photocatalytic process. *J Environ Sci (China)*. **65**: p. 201-222. 2018